

The New Scintillating Fiber Detector of E835 at Fermilab

W. Baldini, D. Bettoni, R. Calabrese, G. Cibinetto, E. Luppi, R. Mussa, M. Negrini, and G. Stancari

Abstract—A cylindrical scintillating fiber detector for the measurement of the polar coordinate θ has been built for experiment E835 at Fermilab. This is the first detector used in a high-energy physics experiment that exploits scintillating fibers and visible light photon counters (VLPCs). It combines the high granularity, flexibility, and fast response of the scintillating fibers with the high quantum efficiency of the VLPCs. Complete results about tracking resolution, detection efficiency, time resolution, long-term stability, and reliability are given.

Index Terms—Charmonium, scintillating fiber detector, tracking system, visible light photon counter (VLPC).

I. INTRODUCTION

EXPERIMENT E835 studies the direct formation of charmonium mesons in antiproton–proton annihilations [1], [2]. The antiproton beam is stored and stochastically cooled in the antiproton accumulator, where it intersects a gaseous hydrogen jet-target in a region of about $5 \times 5 \times 7 \text{ mm}^3$. The E835 detector is a nonmagnetic spectrometer designed to select the electromagnetic decays of the charmonium mesons that include electrons, positrons, and photons. The central detector is symmetric around the beam axis. It has a full azimuthal (ϕ) coverage and a polar angle (θ) acceptance from 10.6° to 70.0° . The E835 apparatus consists of an inner tracking system, a threshold Čerenkov counter, a lead-glass central electromagnetic calorimeter, and a forward electromagnetic calorimeter.

Part of the inner tracking system is a scintillating fiber detector designed to measure the polar angle θ of charged tracks from 15° to 65° . The readout of the detector exploits visible light photon counter (VLPC) semiconductor devices, developed by Rockwell international, with high quantum efficiency (QE) and high gain.¹ Thanks to the VLPCs' fast response, this detector can also be used in first-level trigger logic.

The scintillating fiber detector described in this paper is an upgrade of the one built for run I of E835 (years 1996–1997). This detector was made of two layers of 430 fibers each, read out by latches (Le Croy PCOS III) and, for 61% of the channels, by analog-to-digital converters (ADCs) [3].

For run II of E835 (year 2000), the detector has been substantially improved. The new detector consists of four layers of

fibers, with all channels equipped with both ADC and time-to-digital converter (TDC) readout. This allows a more efficient reconstruction of the charged tracks as well as a better angular resolution.

Given the higher rate of events of E835 run II (almost two times higher than during run I), the TDC readout of each channel provided an important information to recognize events where the “pileup” (i.e., pileup of charge coming from different events) occurs.

II. DETECTOR DESIGN

The new scintillating fiber (SCI-FI) detector, represented in Fig. 1, consists of four layers of 240, 240, 430, and 430 scintillating fibers, respectively, mounted on four coaxial cylindrical supports. Each support is made of acrylic and has a thickness of 3.5 mm, corresponding to 0.9% radiation length at normal incidence.

Each scintillating fiber is wound around one of the four supports (radii of 85.0 mm, 92.0 mm for the inner layers, 144.0 mm and 150.6 mm for the outer ones, respectively).

On the surface of these cylinders, a set of U-shaped grooves has been machined (pitches 1.10 mm, 1.19 mm, 1.10 mm, and 1.15 mm for the four layers, respectively). The depth of the grooves varies linearly with the azimuthal coordinate ϕ , so that the fiber overlaps itself after one turn. To maximize the geometrical acceptance, the grooves of adjacent layers are such that each fiber of one layer covers the “crack” between two fibers in the next layer. Design parameters have been derived from Monte Carlo simulations. The expected total detection efficiency (at least one hit in one of the four layers) is better than 99% for $\theta < 50^\circ$ ($\simeq 0.9$ rad). Requiring one hit in one of the two inner layers and one hit in one of the two outer layers, the expected efficiency is about 99% for $\theta < 45^\circ$ and better than 90% for $\theta < 45^\circ$ ($\simeq 0.75$ rad). This efficiency loss is due to the fact that at large angles, each track crosses a smaller number of fibers and has a lower probability to be detected.

All the fibers used in this detector are Kuraray multicladd.² The scintillating fibers, type SCSF-3HF, have a diameter of 0.835 mm and an average attenuation length of 5.5 m. The scintillating fiber is thermally spliced to a clear fiber, which brings the light to the VLPCs. On the other end of the scintillating fiber, a thin layer of aluminum (thickness ~ 200 nm) has been deposited to increase the light yield by reflecting back the light that otherwise would be lost. To facilitate the operation of connecting the detector to the E835 apparatus, the clear fiber has been separated into two segments (see Fig. 2). The first segment, 2.2 m long, has fibers of the same diameter as the scintillating ones (0.835

Manuscript received October 28, 2000; revised February 23, 2001 and March 26, 2001.

W. Baldini, D. Bettoni, R. Calabrese, G. Cibinetto, M. Negrini, E. Luppi, and G. Stancari are with the Dipartimento di Fisica, Università degli studi di Ferrara, Ferrara 44100, Italy and Sezione di Ferrara, Istituto Nazionale di Fisica Nucleare, Ferrara 44100, Italy (e-mail: baldini@fe.infn.it).

R. Mussa is with the Sezione di Torino, Istituto Nazionale di Fisica Nucleare, Torino 10125, Italy.

Publisher Item Identifier S 0018-9499(01)06979-9.

¹Rockwell International Science Center, Thousand Oaks, CA.

²Kuraray USA, New York, NY.

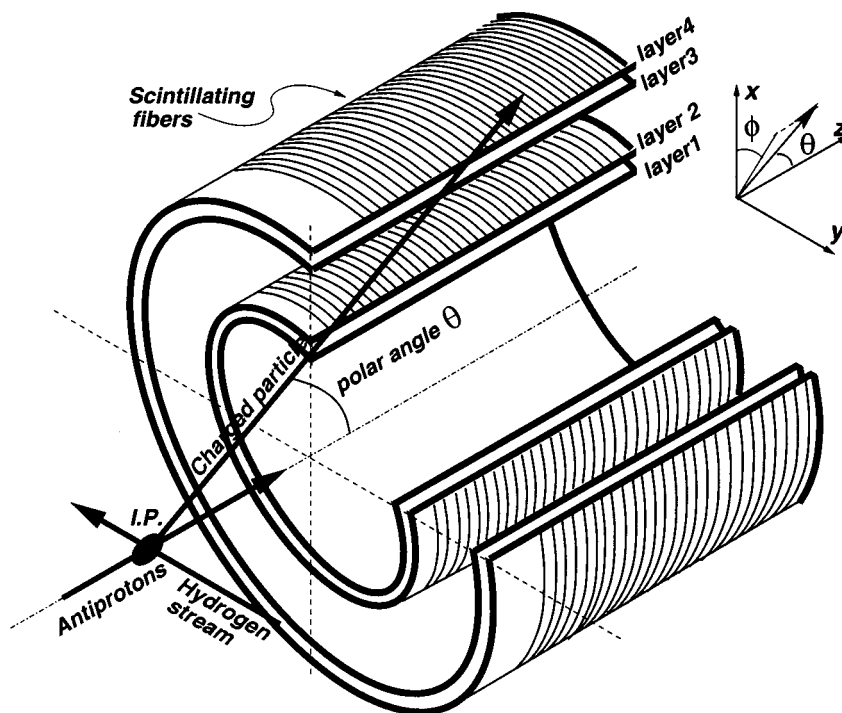


Fig. 1. The geometry of the SCI-FI detector.

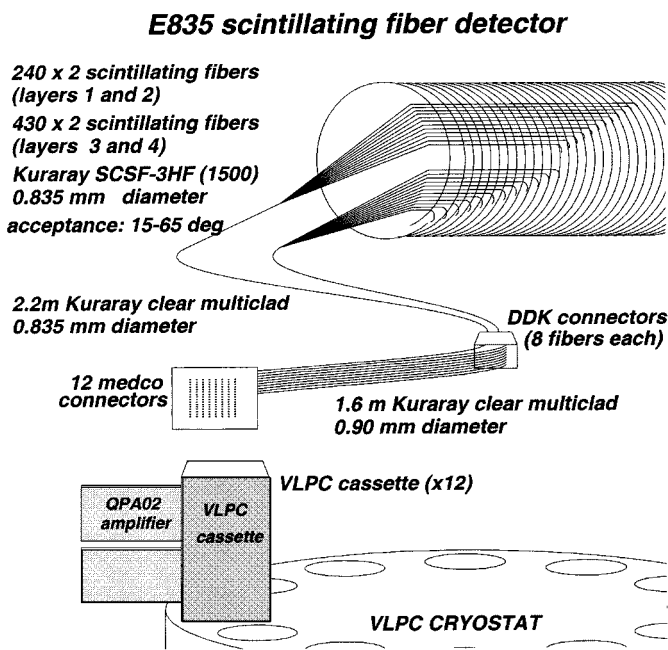


Fig. 2. Schematic view of the SCI-FI detector and of the readout system.

mm). The second segment exploits fibers with a slightly larger diameter (0.900 mm) to reduce the loss of light in the connection. The clear fibers have an average attenuation length of 10.4 m and the loss of light is on the order of 30%.

III. DETECTOR READOUT AND THE CRYOGENIC SYSTEM

The light generated from the scintillating fiber is transformed into an electric signal thanks to the VLPCs (Histe-V), solid-state

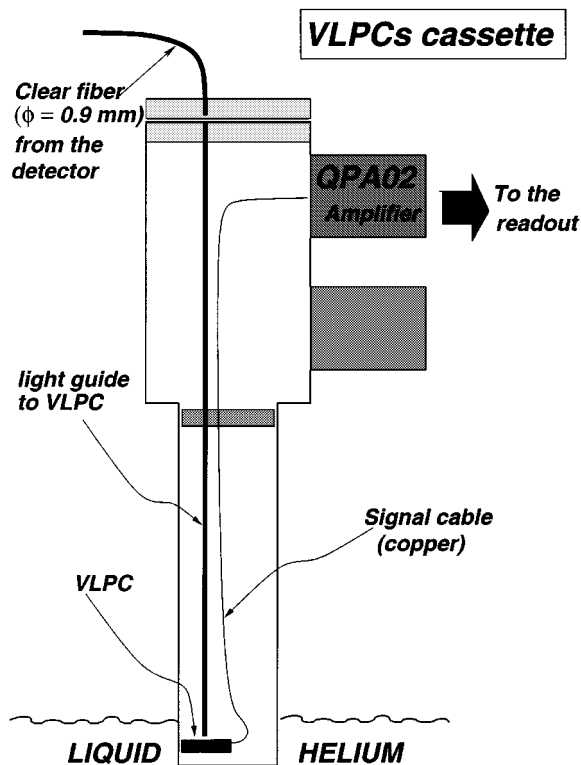


Fig. 3. Schematic view of a VLPC cassette.

photosensitive devices characterized by a very high quantum efficiency in the visible region ($\approx 70\%$ at 550 nm) and gain better than 2×10^4 . To work correctly, the VLPCs have to be kept at a very low temperature (below 10 K). The gain, quantum efficiency, and “dark current” (the thermal noise) of these devices

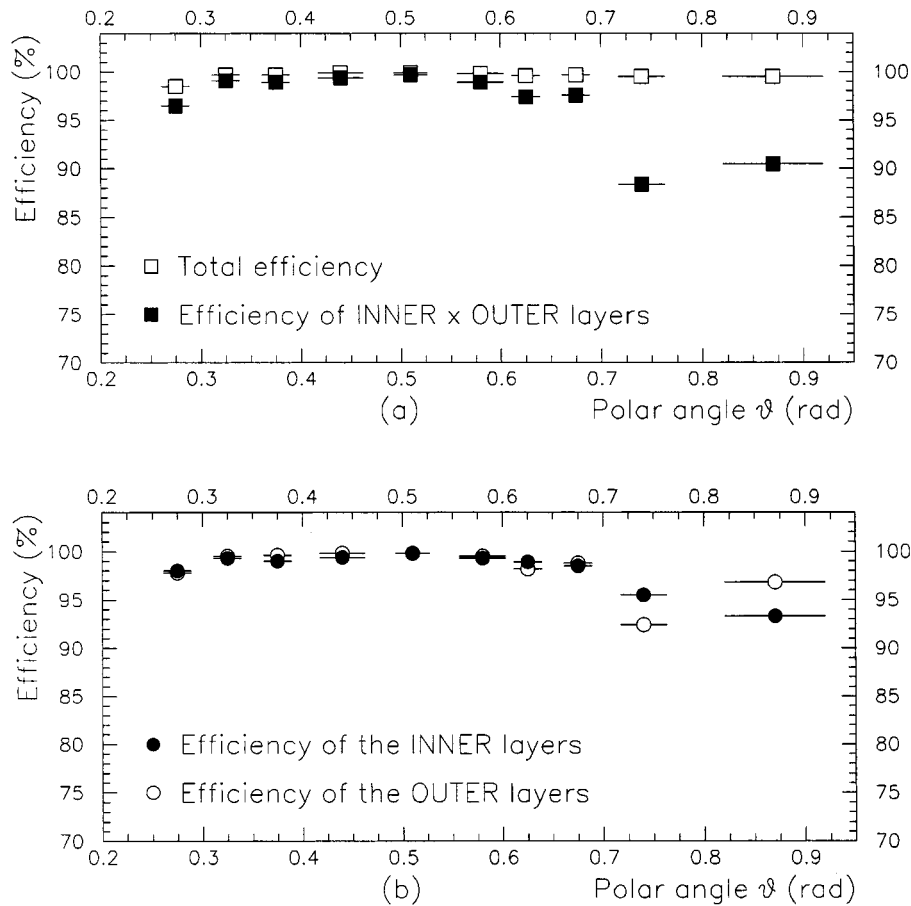


Fig. 4. Detection efficiency of the scintillating fiber detector as a function of θ . (a) Open squares: at least a hit in one of the four layers; solid squares: at least a hit in one of the two inner layers and a hit in one of the two outer layers. (b) Detection efficiency of the inner layers (open circles) and outer layers (solid circles).

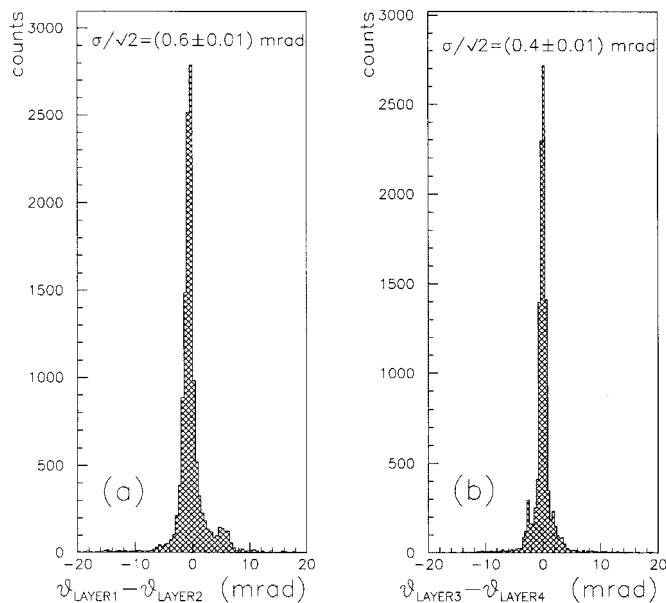


Fig. 5. Intrinsic angular resolution of the (a) inner and (b) outer layers.

depend on the temperature [4]. The optimal working temperature, i.e., the best tradeoff between high-gain QE (but also high dark current) and low dark current (but low-gain QE) was found, after some studies, to be $T = 6.5$ K.

The VLPCs are housed in a “VLPC cassette” (see Fig. 3) custom-made in Fermilab. Its task is to bring the light from the clear fibers to the VLPCs and bring back the electric signal from the VLPCs to the amplifiers, keeping the VLPCs at a temperature of 6.5 K inside a cryostat. Each cassette holds a total of 128 VLPC channels, grouped in 16 arrays of eight VLPC pixels each. The arrays are fixed to a copper support that keeps all the VLPCs at the same temperature.

A liquid helium cryogenic system has been developed, from the Fermilab Cryogenic Group, to refrigerate the 12 VLPCs’ cassettes [6]. The system has been designed to keep the cryostat at a constant temperature in the range of 4.5 K to 15 K. The stability of the temperature, with a set point of 6.5 K, was better than 0.05 K.

The small electric signal generated by the VLPCs is amplified by QPA02 cards, 32-channel high-gain amplifiers (gain ≈ 17 mV/fC) designed and built at Fermilab [9]. After the amplification stage, the signal is sent to discriminator-OR-splitter modules custom-made in Ferrara. These 32-channel modules provide analog and digital output for each input channel, together with the digital OR of all inputs. The analog signal is sent to LeCroy 4300B ADCs, while the digital output is read out by LeCroy 3377 TDCs.

For triggering purposes, the detector has been divided into nine θ regions, corresponding to 19 sets of adjacent fibers (“bundle”). The digital OR of the signals from each bundle is

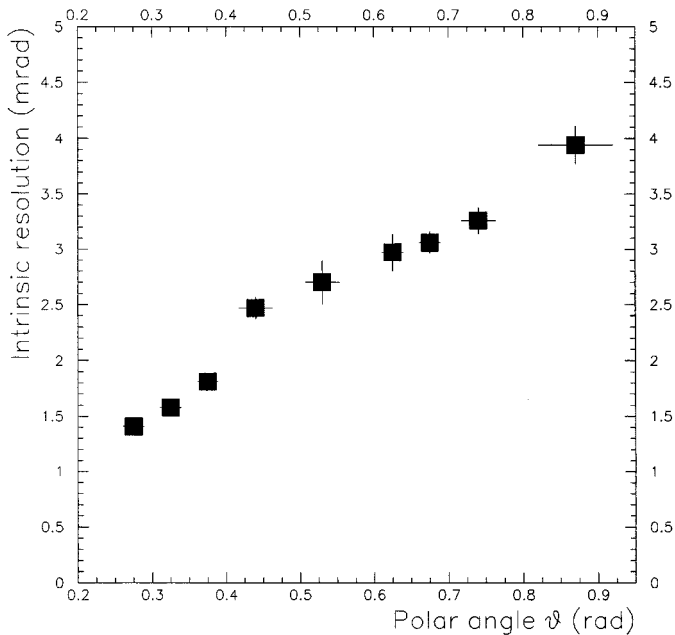


Fig. 6. Overall intrinsic resolution.

also sent to a LeCroy 3377 TDC and to the first-level trigger logic of the experiment (see also Section VIII).

IV. CALIBRATION

The signal generated by a track crossing one fiber, as seen at the input of the discriminator-OR-splitter modules, is typically 180 mV high and 80 ns wide, corresponding to a collected charge of ≈ 0.1 nC.

To obtain, for each VLPC channel, the one-photoelectron (phe) equivalent in ADC counts ($1 = \text{ADC count} = 0.25$ pC), we performed some measurements with a light-emitting diode (LED). We sent a small amount of light to each channel, through the LED, with the setup actually used in the experiment (VLPC cassettes, cryostat, and readout electronics) and looked at the charge corresponding to the 1-phe peak. The charge, in ADC counts, generated by a minimum ionizing particle (mip) was obtained studying a high-statistics hadronic sample of punch-through tracks selected through the electromagnetic calorimeter. Combining the two, we have the number of “phe per mip.”

V. DETECTION EFFICIENCY

We measured the detection efficiency by using a sample of (~ 15 000) elastic $\bar{p}p$ tracks in the energy range of 3.385–3.530 GeV in the center of mass that corresponds to the χ_0 and 1P_1 states of charmonium. The elastic $\bar{p}p$ event was detected by the central calorimeter. For each track, we then looked for an associated hit in the scintillating fiber detector within a window of ± 50 mrad. We defined a hit as an on-time signal in the TDC and a signal above a given threshold (about three photoelectrons) in the corresponding ADC. The results are shown in Fig. 4. The drop in the efficiency at $\theta > 0.75$ rad is due to an expected decrease in the geometrical acceptance of the detector starting from that angle (see Section II).

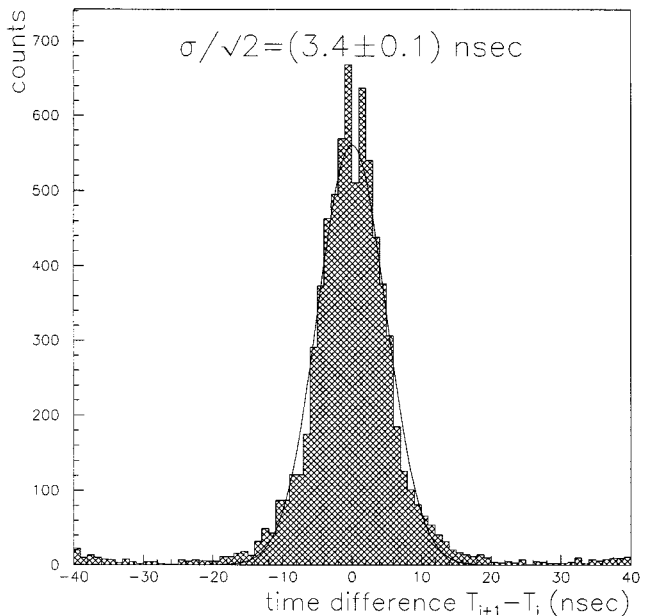


Fig. 7. Overall time resolution.

VI. ANGULAR RESOLUTION

The scintillating fiber detector is by far the one with the best spatial resolution in our apparatus. For this reason, we can only measure an “intrinsic” tracking resolution, i.e., the standard deviation (divided by $\sqrt{2}$) of the distribution of the differences $\theta_i - \theta_j$, where, for a given track, θ_i and θ_j are the polar angles measured by two different layers. The factor $1/\sqrt{2}$ is due to the fact that the measured distribution includes the resolutions of two layers. The angular resolution, averaged over all polar angles, comes out to be 0.6 ± 0.1 mrad for the two inner layers and 0.4 ± 0.1 mrad for the outer ones, as shown in Fig. 5. The excess on the tails of the distributions is due to the discrete nature of the single-layer measurement. At large angles ($\theta > 0.6$ rad), a track can hit a single fiber, say, N , in layer 1 and fiber $N+1$ in layer 2. When this occurs, the two single-layer measurements can differ by a few mrad, corresponding to the angular distance between two adjacent fibers.

Fig. 6 shows the overall intrinsic resolution calculated from the difference between the average of the angles measured by the two inner and the two outer layers. The overall intrinsic resolution is limited by the multiple scattering effect that occurs in the material in between them, as we have verified with a Monte Carlo simulation.

VII. TIMING RESOLUTION

To determine the intrinsic time resolution of the detector, we selected those tracks that hit exactly two adjacent fibers. We define the time resolution as the standard deviation, divided by $\sqrt{2}$, of the distribution of the variable $t_{i+1} - t_i$, when the same track crosses the i th and the $(i+1)$ th fibers. The factor $1/\sqrt{2}$ takes into account the fact that the measured distribution incorporate the time resolutions of two fibers. Fig. 7. shows the overall time distribution of the detector; it comes out to be 3.4 ± 0.1 ns and is mostly due to the decay time of the scintillator.

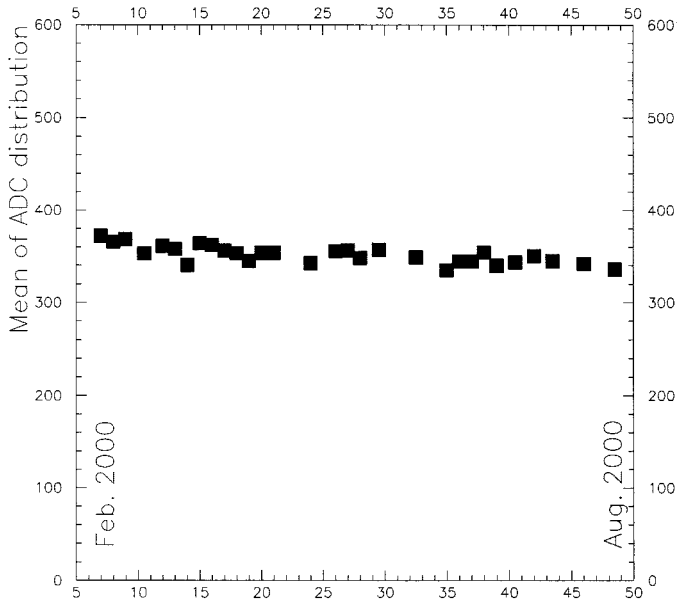


Fig. 8. Long-term stability of the signal. Mean of the ADC counts distribution as a function of time for a typical fiber (a “stack” correspond to $\approx 1/2$ week).

VIII. FIRST-LEVEL TRIGGER

Thanks to the fast response and to the very good time resolution, the scintillating fiber detector is also used in the first-level trigger. The coincidence of sets of fiber bundles can in fact select very efficiently events with the right polar kinematic. In particular, it has been used to study the decay of the charmonium states into the $\phi\phi \rightarrow K^+K^-K^+K^-$ and elastic $\bar{p}p$ channel. This first-level selection reduces the rate to affordable values for the data acquisition system: ~ 100 Hz (for an instantaneous luminosity of $1 \times 10^{31} \text{ cm}^{-2} \text{ s}^{-1}$) for the $\bar{p}p$ trigger and < 1000 Hz for the $\phi\phi$ trigger.

IX. LONG-TERM STABILITY

The stability of the signal from the detector has been checked throughout the data taking. For each channel, we fitted the ADC count distribution with a Gaussian and looked at the mean value as a function of time. Typical results are shown in Fig. 8. During the data-taking period (~ 6 months), the signal was stable, typically within a few percent. The overall variation was smaller than 10%.

X. RELIABILITY OF THE EQUIPMENT

During the data taking of E835 run II, the cryogenic system worked very efficiently, keeping the VLPCs at a temperature constant within ± 0.05 K. Several warmups occurred. Most of them were scheduled shutdowns or power outages and did not affect the data taking. Despite the fact that the temperature rose—in one case up to the room temperature—the loss of

channels was limited to a few percent. This was possible thanks to special care taken to avoid any humidity infiltration into the VLPC’s volume, which is the major cause of oxidation (and subsequent breakage) of the very fragile signal connections. At the beginning of the data taking, 30 dead channels, out of 1340 (2.2%), were not working. At the end, we had a total of 61 dead channels (4.5%). This small loss of channels did not cause any observable change in the performances of the detector.

XI. CONCLUSIONS

In this paper, we presented the results of the first detector used in a high-energy-physics experiment that exploits scintillating fibers and visible light photon counters. It is a unique detector because it combines a good tracking performance (resolution better than 1 mrad, detection efficiency $\approx 98.0\%$), fast first-level trigger characteristics (time spread better than 4 ns), and good stability of the signal over time.

ACKNOWLEDGMENT

The authors wish to thank the Fermilab Particle Physics Division, the Cryogenic Group, and all the E835 collaborators for their valuable support. In particular, the authors want to thank S. Pordes (Fermilab Particle Physics Division) and R. Schmitt (PPD engineering). Special thanks go to the Ferrara technical staff—V. Carassiti, S. Chiozzi, A. Cotta, L. Landi, L. Milano, and M. Melchiorri—for their help and cooperation.

REFERENCES

- [1] T. Armstrong, D. Bettoni, C. Biino, G. Borreani, D. Broemmelsielk, and A. Buzzo, *et al.*, “Proposal to continue the study of charmonium spectroscopy in proton–antiproton annihilations,” (E760 Collaboration), Fermilab proposal P-835-REV, Sept. 1992.
- [2] R. Cester and P. A. Rapidis, “Charmonium formation in $p\bar{p}$ annihilations,” *Ann. Rev. Nucl. Sci.*, vol. 44, pp. 329–371, 1994.
- [3] M. Ambrogiani, W. Baldini, D. Bettoni, M. Bombonati, D. Bonsi, and R. Calabrese, *et al.*, “Construction and performances of a cylindrical scintillating fiber detector for experiment E835 at Fermilab,” *IEEE Trans. Nucl. Sci.*, vol. 44, pp. 460–463, June 1997.
- [4] G. B. Turner, M. G. Stapelbroek, M. D. Petroff, E. W. Atkins, and H. H. Hogue, “Visible light photons counters for scintillating fibers applications: Characteristics and performance,” in *Proc. SCIFI’93*, 1995, pp. 613–620.
- [5] M. Ambrogiani, W. Baldini, D. Bettoni, R. Calabrese, E. Luppi, R. Mussa, and G. Stancari, “The Fermilab E835 scintillating fiber detector,” *Nucl. Phys. B (Proc. Suppl.)*, vol. 78, pp. 479–483, 1999.
- [6] T. H. Gasteyer and P. D. Wheelwright, “Performance and control of a cryogenic system cooling 1152 VLPC channels,” *Adv. Cryo. Eng.*, vol. 43A, pp. 549–556, 1998.
- [7] M. Ambrogiani, W. Baldini, D. Bettoni, R. Calabrese, E. Luppi, R. Mussa, and G. Stancari, “Performances measurements of Histe-V VLPC photon detector for E835 at FNAL,” in *Proc. SCIFI’97*, 1999, pp. 355–360.
- [8] M. Ambrogiani, W. Baldini, D. Bettoni, R. Calabrese, E. Luppi, R. Mussa, and G. Stancari, “Results from the E835 scintillating fiber detector,” *Nucl. Instrum. Meth.*, vol. A419, pp. 632–636, 1998.
- [9] R. J. Yarema and T. Zimmerman, “A high speed, high gain preamplifier system for silicon strip detectors,” *IEEE Trans. Nucl. Sci.*, vol. 37, pp. 439–443, Apr. 1990.